Magnetic Resonance Fingerprinting with Chemical Exchange (MRF-X) for Quantification of Subvoxel T1, T2, Volume Fraction, and Exchange Rate

Jesse I. Hamilton[1], Anagha Deshmane[1], Stephanie Hougen[2], Mark Griswold[1,3], and Nicole Seiberlich[1,3]
[1]*Biomedical Engineering, Case Western Reserve University, Cleveland, OH, United States,* [2]*Physics, Case Western Reserve University, Cleveland, OH, United States,* [3]*Radiology, Case Western Reserve University, Cleveland, OH, United States*

TARGET AUDIENCE: Clinicians and MR scientists interested in MRF, subvoxel parameter mapping, and chemical exchange modeling.

PURPOSE: It is assumed in conventional parameter mapping that chemical exchange occurs on a time scale much faster than the rate at which measurements are performed[1], which is usually on the order of T_1 or T_2. However, methods that collect information on significantly shorter time scales are able to probe the effects of chemical exchange[2]. MR Fingerprinting (MRF)[3,4] potentially satisfies this property by collecting information every T_R, or every 6-20ms. This work presents a new technique termed MRF-X that models the physics of chemical exchange when building the MRF dictionary to create subvoxel maps of T_1, T_2, volume fraction, and exchange rate in two-compartment voxels. **METHODS:** Simulations were performed using the Bloch-McConnell equations[5], which are modified forms of the Bloch equations for two exchanging compartments A and B. There are a total of six important parameters, including four relaxation time constants $(T_1^A, T_2^A, T_1^B, T_2^B)$, the exchange rate k_{AB} from compartment A to B, and the volume fraction ρ_A of species A. It should be noted that $\rho_B = 1 - \rho_A$ and that under steady state conditions $\frac{k_{BA}}{k_{AB}} = \frac{\rho_A}{\rho_B}$. In a first simulation, the ability of MRF-X to differentiate volume fraction and exchange conditions that would be indistinguishable using standard parameter mapping was explored. Two pairs of effective T_1 and T_2 values were chosen: T_1/T_2=824/63ms and T_1/T_2=1453/46ms. For each pair, three cases were simulated with fast, moderate, and slow exchange rates ($k_{AB} = 10^3, 1,$ and $10^{-3} s^{-1}$ respectively) using subvoxel T_1, T_2, and volume fractions selected to yield the desired apparent T_1 and T_2 combinations. These two-compartment parameters are summarized in the tables in Figure 1. Standard parameter mapping sequences (inversion recovery spin echo with inversion times between 20-3000ms and an echo time 50ms for T_1, and spin echo with echo times between 0-200ms for T_2 with full relaxation between RF pulses) were simulated to verify that these combinations all produce a perfect monoexponential fits for T_1 and T_2 despite actual differences in the subvoxel parameters and exchange rates. Signal evolutions for these six cases were also generated using a FISP-based MRF-X sequence designed for volume fraction and exchange sensitivity with 1000 RF pulses, pseudorandom flip angles (0-70°) and TRs (6-20ms), and an inversion pulse with TI=500ms after every 200 RF pulses. A second simulation was performed to demonstrate that MRF-X can be used to generate subvoxel parameter maps with dictionary mapping, as in standard MRF. A digital phantom was generated with nine regions corresponding to effective T_1/T_2=824/63ms, T_1/T_2=1030/84ms, and T_1/T_2=1453/46ms each with fast, moderate, and slow exchange cases. Both the standard mapping and MRF-X sequences were simulated using a fully-sampled Cartesian trajectory with random Gaussian noise (SNR=0.3%) added in k-space. A large six-dimensional dictionary was generated for pattern matching with a total of 10,800 entries: T_1^A: 350-832ms, T_1^B: 1385-3000ms, T_2^A: 30-41ms, T_2^B: 50-150ms, $k_{AB} = \{10^{-3}, 1, 10^3\ s^{-1}\}$, and ρ_A: 14-60%. **RESULTS:** Figure 1 shows MRF-X signal evolutions for the three pairs of effective T_1 and T_2 values described above with differing chemical exchange rates. The MRF-X signals with different subvoxel parameters produce unique time courses even though they yield the same apparent T_1 and T_2 with conventional mapping sequences. Figure 2 (left) shows the ground truth images from the digital phantom study. Nine simulated vials are shown with exchange rates of $10^3, 1,$ and $10^{-3} s^{-1}$ going from left to right. Conventional methods give apparent monoexponential T_1 and T_2 pairs in each row (T_1/T_2=824/63ms top row, T_1/T_2=1030/84ms middle row, and T_1/T_2=1453/46ms bottom row) despite actual differences in the underlying subvoxel parameters (center). However, MRF-X was able to accurately quantify the subvoxel parameters with minor errors due to the added noise (right). **DISCUSSION:** MRF-X has been proposed to measure T_1, T_2, volume fraction, and exchange rate in two-compartment voxels. There are numerous applications that would benefit from the ability to measure these properties of tissue microstructure directly. Quantification of myocardial extracellular volume fraction, which is useful in evaluating fibrotic disease, is currently calculated indirectly using pre- and post-contrast T_1 measurements of blood and myocardium. However, MRF-X may be able to measure ECV directly in a single scan without contrast administration. More generally, it may be possible measure properties related to cell membrane integrity and transport, areas not easily accessible to MRI. **CONCLUSION**: MRF-X has been introduced for measuring subvoxel 2D relaxation parameters, volume fraction, and chemical exchange rate.

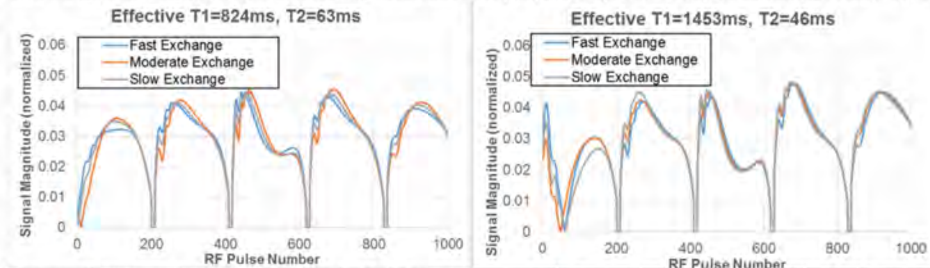

Exchange Regime	Exchange Rate (s^{-1})	T_1^A (ms)	T_2^A (ms)	T_1^B (ms)	T_2^B (ms)	Fraction A	Exchange Regime	Exchange Rate (s^{-1})	T_1^A (ms)	T_2^A (ms)	T_1^B (ms)	T_2^B (ms)	Fraction A
Fast	10^3	350	30	1385	92	23%	Fast	10^3	350	30	3000	50	14%
Moderate	1	350	30	1400	95	46%	Moderate	1	800	30	3000	70	56%
Slow	10^{-3}	350	30	1400	120	60%	Slow	10^{-3}	832	30	2930	67	55%

***Figure 1**. MRF-X signal evolutions are shown for two pairs of effective T_1 and T_2 values, each with cases for fast, moderate, and slow exchange. In each panel the MRF-X signals appear different, although standard mapping sequences would result in a monoexponential relaxation parameter fit.*

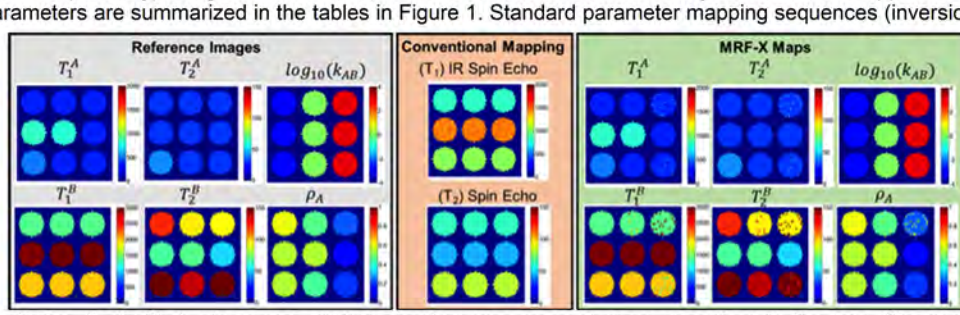

***Figure 2**. (Left) A nine-region digital phantom was generated as described in the text. Standard mapping sequences (center) only match a single effective T_1 and T_2 value in each region despite differences in subvoxel parameters. MRF-X (right) is able to map subvoxel relaxation parameters, exchange rate, and volume fraction using an optimized sequence and dictionary mapping.*

ACKNOWLEDGMENTS*: Siemens Medical Solutions; NIH T32EB007509, R00EB011527, RO1HL09455, R01EB016728.*

REFERENCES: [1]Donahue K, et al. *JMRI*, 1997. [2]Deoni S, et al. *JMRI* 2008. [3]Ma D, et al. *Nature*, 2013. [4]Jiang Y, et al. MRM 2014. *In press.* [5]McConnell HM. *J Chem Phys*, 1958.